International Journal on Interactive Design and Manufacturing (IJIDeM)
https://doi.org/10.1007/s12008-023-01218-7

ORIGINAL PAPER

Numerical comparison of advanced high strength steels forming limit curve using Banabic and Nakazima tests

Roberto Matheus De Araujo Bornancin[1] · Chetan P Nikhare[2] · Paulo Victor Prestes Marcondes[1]

Received: 6 December 2022 / Accepted: 20 January 2023

Abstract
With the increase of government regulation, pressure to reduce environmental impact, fuel consumption, and safety improvements, the steelmaking industry has developed Advanced High-Strength Steels. However, the application of these steels depends on the knowledge of mechanical properties and parameters of the forming processes. Forming limit curve (FLC) is an important tool used to evaluate the formability of sheet metal. The aim of this study is to modify and analyze the Banabic method to the standards of DIN EN ISO 12004-2 and then comparing it to the Nakazima test using first generation Dual-phase 600. For this purpose, numerical simulations with experimental data verification, the differences of both methods were performed. Based on finite element simulations the adapted Banabic method resulted in uniform punch force and strain profile than Nakazima specimens. The Banabic test method provides greater strain, stress distribution and maximum strain values closer to the punch pole in their specimens. Therefore, modified Banabic method has advantages over the Nakazima test, as to induce a fracture behavior closer to the punch pole in the same friction conditions and easier machining of specimens.

Keywords Forming limit curve · Advanced High Strength-Steels · Numerical analysis · Nakazima test · Banabic model

1 Introduction

The automotive industry has been presenting several modifications in the materials used in vehicles production due to government regulations, high competition, consumer preferences and financial market. In addition, these companies seek to reduce the cost of materials in synergy with more manufacturability, greater energy absorption during collision, less energy consumption and lower emission of greenhouse gases in the lifecycle [1–5].

In addition to the challenges that internal combustion models face, companies that produce electric vehicles must face other types of requirements as popular adoption increases [6, 7]. Among these, the reduction of electrical consumption, greater autonomy of route through the improvement of the kinetic energy recovery system, efficiency in the production and acquisition of the raw material of the batteries, which currently have Lithium as the main element, considered by Harlow as "white oil" [8]. Therefore, the class of electric as well as internal combustion vehicles presents challenges inherent to their production in synergy with society's expectations. However, body weight reduction is sought after by both classes. To promote this, the steel industry has developed advanced high-strength steels (AHSS) that have a multiphase microstructure and, in some types, greater formability than conventional steels, such as high-strength low-alloy steel [1]. However, in order to meet these requirements, it is necessary to consider from manufacturing to recycling the material selected for the project, since each element of its chemical composition presents an energy expenditure for manufacture [1, 3].

AHSS are multiphase that can present more than one deformation mechanism [1, 3]. For example, Dual-phase (DP) steels exhibit a ferritic matrix, which is generally ductile, with a secondary phase of martensite in the form of islands, which presents high strength and low ductility, a condition that provides greater ductility and mechanical strength in the conformation when compared to conventional steels [1–3, 5]. In DP steels the martensite secondary phase can vary from 10 to 40% of the total volume [9–12].

✉ Chetan P Nikhare
cpn10@psu.edu

[1] UFPR – Universidade Federal do Paraná, Curitiba, Brazil

[2] Penn State Erie – The Behrend College, Erie, PA, USA

Table 1 Steel DP 600 Mechanical properties [24]

Yield Strength (MPa)	Tensile Strength (MPa)	Elongation (%)	Young modulus (GPa)	Strain hardening coefficient	R0	R45	R90
410	640	28.5	207	0.188	0.6739	1.0354	0.9977

These steels may have bainite, retained austenite and pearlite in their microstructure. However, these last two phases are usually in small quantities and, consequently, do not change the mechanical properties of these steels significantly [13]. It is essential to know the properties and forming limits of AHSS as precisely as possible of practical conditions to reduce stamping problems [12, 14]. Furthermore, Abspoel et al. [15] and Banabic et al. [16] corroborate that the use of the forming limit curve (FLC) is an important and widely used tool to determine the sheets forming limits of steel that are used in automobiles.

The FLC was partially developed by Keeler [17], who described a strain map, relating the major and minor positive strains, which made it possible to determine the limits of sheet forming in the stretched state in a punch. Later, the curve was extended by Goodwin [18], who evaluated the minor negative strain, thus allowing the evaluation of deep drawing and uniaxial stress states. The FLC indicates the amount by which a material can be deformed to the point of fracture, with the combination of plane strain, uniaxial strain, and stretching states. The FLC has three deformation zones that must be analyzed before forming: the safe zone, where failure during forming is not expected; the critical zone, which the probability of necking is high; the failure zone, where there is an increased probability of sheet rupture. The FLC is determined by measuring the deformations in the plane along predefined directions, followed by a data interpolation that allows to obtain the sheet forming limits, to avoid necking. There are several studies that guide which circles or ellipses, depending on the type of deformation state, which should be analyzed in relation to the fracture region. Gipiela et al. [19] measured the mesh on the opposite side of the crack, according to the numbered circles, indicating the material's rupture limits. However, Hecker [20] measures the circles or ellipses on the rupture site, a condition that makes it possible to trace, in addition to the rupture deformations, necking and the values considered safe in conformation. Several methods have been developed for FLCs determination. Among the experimental tests, the Nakazima and Marciniak methods are more common for laboratory tests, which can be determined following the standards of ISO 12004-2 [21]. According to ISO 12004-2 [22], the Nakazima test consists of a hemispherical punch that varies from 98 to 102 mm in diameter, a die with a radius in the range of 5 to 10 mm, blank holder with drawbead and the specimen. The Marciniak test, on the other hand, consists of a cylindrical punch, generally 100 mm in diameter with a 10 mm chamfer, a 20 mm radius die, a plate press with drawbead, a blank for the specimen and a carrier blank. In both tests, the specimens are used that are 190 to 200 mm length, 0.3 to 4 mm thickness and different widths, in order to verify the flat, uniaxial, embedded and stretching states of deformation. The geometry of the specimen, for steel, can be circular or rectangular, have a notch with a radius between 20 and 30 mm and an axis length of 25 to 50 mm.

Banabic et al. [16], in order to reduce the tribological effects between the punch and the sheet, developed a new experimental method based on the hydraulic expansion test, which allows the evaluation of strain states in metallic materials. Unlike the Nakazima and Marciniak test, in which the specimens are deformed by a punch, in the test by Banabic et al. [16] these are deformed by a hydraulic fluid, like the hydraulic expansion test but with the addition of a carrier blank between the fluid and the specimen. However, limited studies are performed without hydraulic pressure. This work aims make a new forming limit curve test based on Banabic Nakazima and Marciniak test. For that, numerical analysis was carried out with DP 600 steel studying the true major strain, thickness distribution and punch force vs. stroke profiles.

2 Materials and methods

The mechanical properties of the DP600 steel with 2 mm thickness used in this study, come from the experimental tests carried out by Chemin Filho [23]. However, in the numerical simulations that were performed in Abaqus Explicit, the friction between the tooling and the sheet was controlled, so it was not necessary to include lubricants in the Nakazima test and carrier blanks (CBs) in the adapted Banabic test, a condition that in practical experiments should be used to mitigate tribological effects.

2.1 Materials description

The tensile tests followed the NBR 6673 standard [21], in order to determine the stress-strain curve, strain hardening coefficient, anisotropy (R), elongation, yield strength, tensile strength in the rolling directions of 0º, 45º and 90º of the DP 600 steel. Table 1 presents the mechanical properties and Fig. 1 the stress-strain curve of this steel.

The mechanical properties were entered in Abaqus in order to describe the elastic and plastic behavior of the material. However, to represent the plastic anisotropic behavior

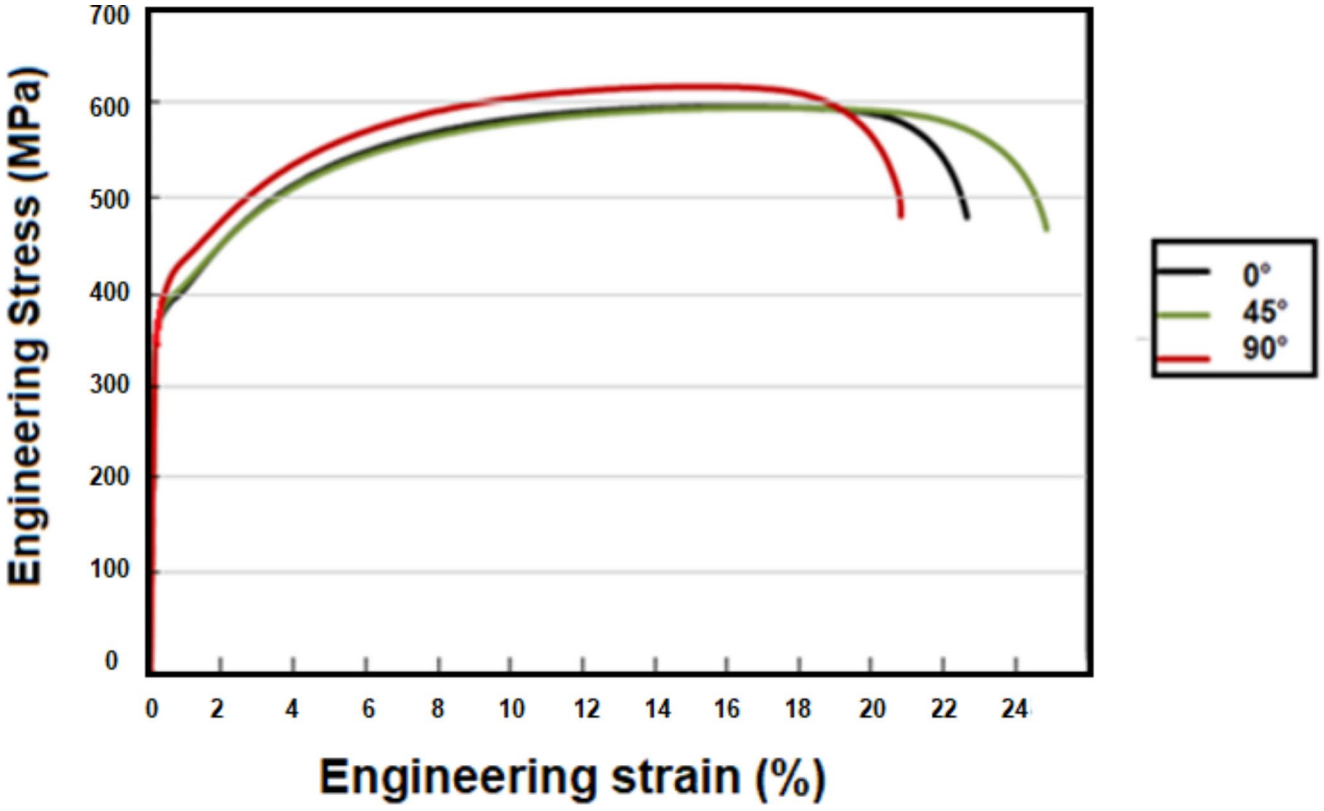

Fig. 1 Strain stress curve rolling direction steel DP 600 [23]

Fig. 2 DP 600 steel forming limit curve [25]

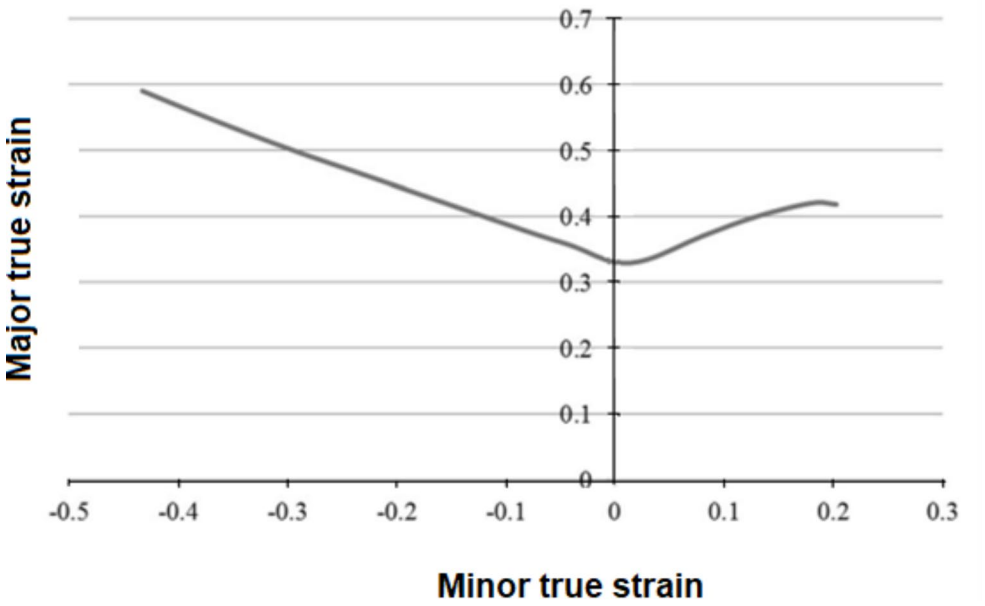

of the material, the Hill 48's criteria was used. In addition, to simulate from the moment of necking to failure of the DP 600 steel, the forming limit curve of DP600 steel was used as shown in Fig. 2.

2.2 Modified banabic model and development computational model

Although the tooling for both analyzed methods is the same as illustrated in Fig. 3, the specimen design is different. To compare the specimen of modified Banabic and Nakazima,

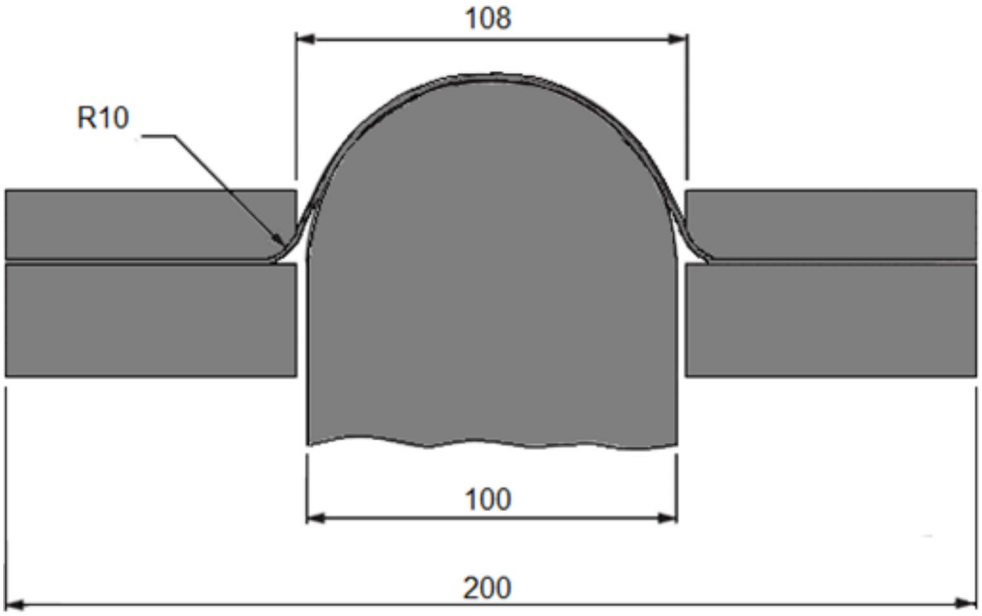

Fig. 3 Tool design used in the numerical simulations

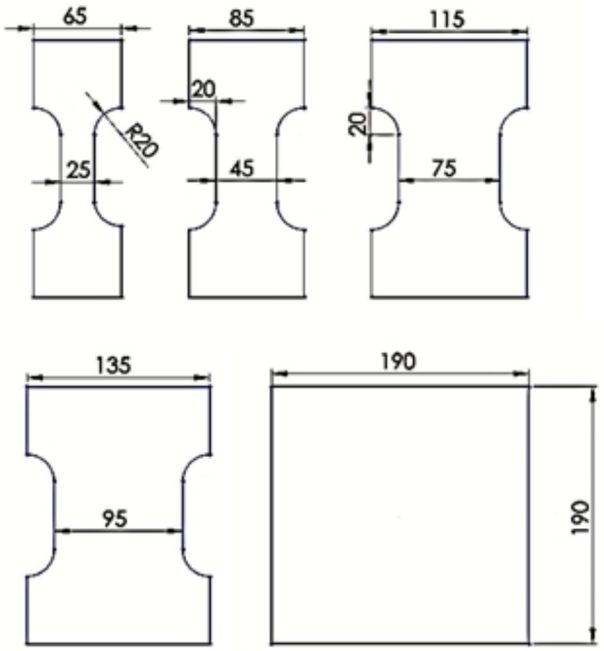

Fig. 4 Specimens used in the simulations

5 specimens were used for each method, which are shown in Figs. 4 and 5, respectively. To accommodate the Banabic specimens in the tooling, all dimensions of the Banabic specimen geometries were increased proportionally, based on the originals, in the range of 5 to 6% to round off the values to facilitate machining or cutting in future practical tests.

The Banabic method that was adapted in the present study is based on the experimental Nakazima and Banabic test. The specimen was developed in the simulations based on the test by Banabic et al. [16], which have two symmetrical holes, which, according to their diameter, allow measuring the limits of conformation of a deformation state predominant in the rupture region.

In the case of practical application in the laboratory (not part of this study) 5 specimen configurations with 3 samples each are used, that allow measuring the limits of conformation for the conditions of deep drawing, uniaxial strain, plane strain, intermediate biaxial stretching, and equi-biaxial stretching. In addition, the carriers' blanks are positioned below the specimen, similar to the Marciniak test, to improve the distribution of the force transmitted by the punch and have no holes with a circular section with an external diameter of 190 mm. The experimental tests were developed based on DIN EN ISO 12004-2 [22], i.e., the specimen is deformed until their rupture. The diameter of the etch circles must be between 1 and 2.5 times the specimen thickness. The carrier blank must be at least 80% the thickness of the specimen. For steels, the specimen were cut perpendicular to the rolling direction, the punch advance speed is 1.5 mm/s, the test temperature must be close to 23ºC, the carrier blank cannot break before the specimen, the rupture site must be close to the top of the specimen, the strain measurements can be done by means of a camera, optical microscope or other measuring devices, such as a caliper.

Given the description of this adaptation and the definition of the properties of DP 600 steel in Abaqus, 2 different models were developed, in order to represent the practical conditions, the first being to analyze the behavior of the material in the Nakazima test and the second the adapted Banabic.

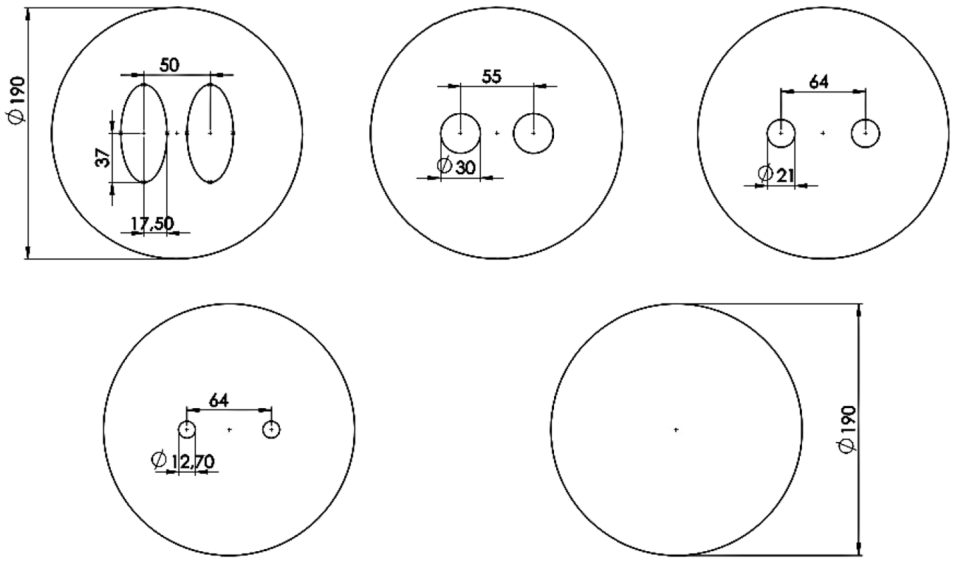

Fig. 5 Banabic modified test specimens used in the numerical simulation

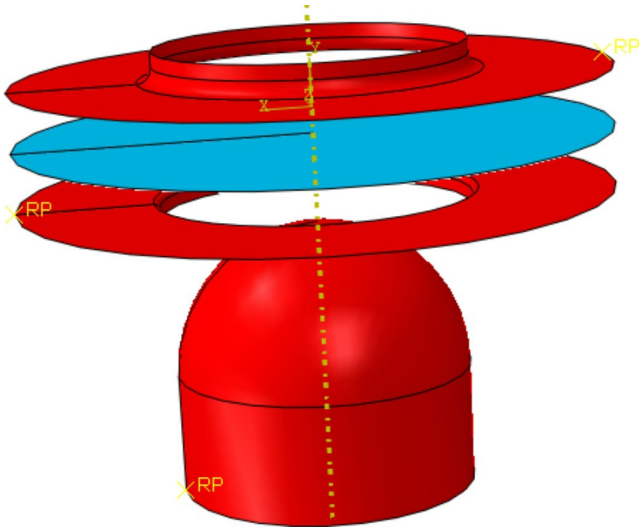

Fig. 6 Tooling assembly configuration of the numerical analysis used in Abaqus

The relationship between force and punch displacement and for the comparison their respective strain profiles, thickness and true major strain were analyzed. In order to reduce the computational processing time, all the tooling was developed in shell mode, with the blank, punch and die as analytically rigid and the blank as deformable, the positioning of these elements are illustrated in Fig. 6. In all specimen of Nakazima and of adapted Banabic, S4R shell emelents with 5 integration points were used through the thickness. The square-shaped mesh with a nodal distance of 1 mm with reduced integration by 4 points was used. For tribological conditions of contact between the bodies, the friction coefficient was set at 0.12 which was verified after comparing the force-displacement curve with experiment.

Each simulation consisted of 3 steps, with an explicit dynamic configuration. In the first step, for the blank holder to advance and apply a load of 200 kN. The second to trigger the punch stroke. The third stop the punch stroke immediately after the failure criterion, from Eq. 1, reaches a value equal to 1. The movement restrictions of the punch and the blank, were applied in the x and z directions and the die was clamped.

$$\omega_{FLD} = \frac{\epsilon_1}{\epsilon_1^{FLD}} \tag{1}$$

3 Results and discussion

The strain profile data of each specimen are illustrated at the moment of rupture, which occurred when Eq. 1 of the FLD failure criterion, in the Abaqus reached the value of 1. In Fig. 7a-e, presents the thickness at failure together with the anisotropic behavior of the specimen (S) of the Nakazima methods. It shows that the fracture occurred in the regions between the die radius and pole punch. The same condition can be seen from Fig. 8a-e for the adapted Banabic method. As seen, the samples of Banabic modified method fractured in the region more close on the pole punch than Nakazima test.

Figure 9 shows the displacement as a function of the punching force of the stretching specimens resulting from the experimental tests carried out by Chemin Filho [23] for the blank holder force of 570 kN and the simulation carried out in Abaqus for S5 with 570 kN to validate the model. It is

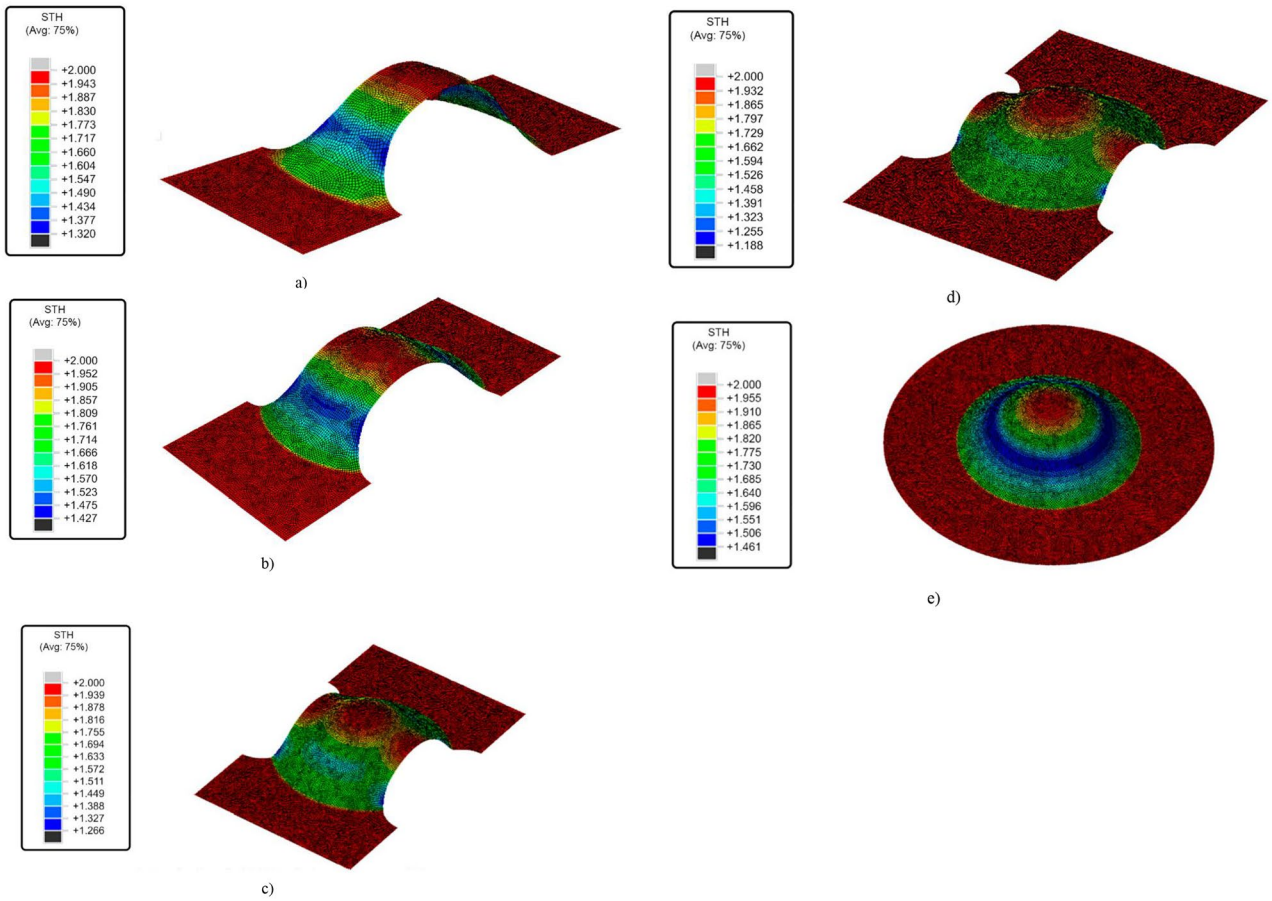

Fig. 7 Thickness profile of simulated from Nakazima test (a) S1, (b) S2, (c) S3, (d) S4 and (e) S5

noted that the profile matches closely with the experimental result.

Figures 10 and 11 show the punch stroke force relationship of the simulations performed for the Nakazima and adapted Banabic tests, respectively. It is noted that the adapted Banabic specimens, in general, present a higher maximum load for rupture and do not present proportionality of maximum force increase in relation to the test sequence. The difference in displacement from the punch to rupture is smaller when compared to the Nakazima profiles. Therefore, under practical conditions, the machine used in the Nakazima test can be used for the modified Banabic method.

.

In Figs. 12 and 13 the strain profiles of the specimens used in the Nakazima and adapted Banabic tests simulations are presented, respectively. The profiles present the distribution of the greatest true deformation in the sheet in relation to the die radius and the punch pole, that is, it indicates the true greatest strain in the region of the die radius, in the intermediate zone and in the punch pole.

Therefore, for the Nakazima test, it was possible to verify that specimen, which has predominant uniaxial strain, fractured closer to the punch pole and presented greater true strain than S5, which has the stretching strain state as predominant, conditions already expected according to plasticity theory. On the other hand, specimens 2, 3 and 4, due to the presence of the states of plane, uniaxial strain and stretching simultaneously, are located in intermediate regions between specimen 1 and 5.

The S1 of the adapted Banabic method presented the greatest true strain peak closer to the punch pole than the sample 1 of Nakazima, being 0.44 and 0.33, respectively. Behavior that can be verified in Fig. 14, with both exhibiting the state of uniaxial strain as predominant during the advance of the punch until rupture, a factor that is possible to verify due to the compressive forces in the region of smaller true strain and stress in the region of greater true strain, facilitating the planar slip in this direction.

The S2 of both methods resulted in relatively similar strain profiles, as shown in Fig. 15. However, the peak of the modified Banabic method was higher, about 0.33, and closer to the punch pole than that of Nakazima. Unlike the S1 of

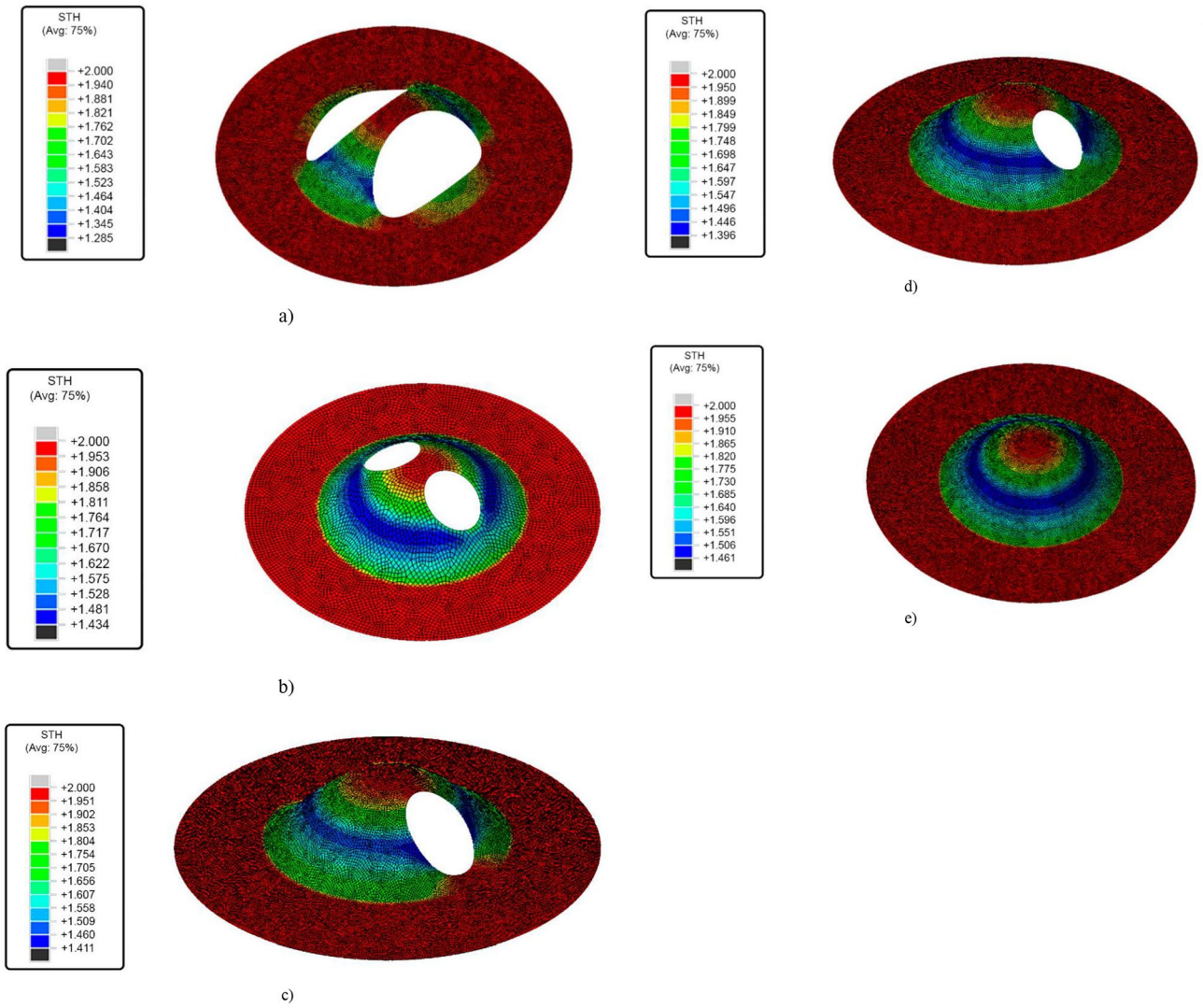

Fig. 8 Thickness profile of simulated from adapted Banabic test (a) S1, (b) S2, (c) S3, (d) S4 and (e) S5

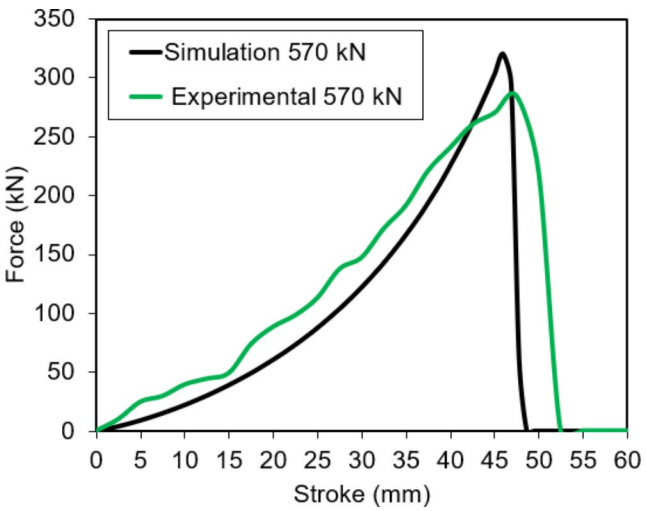

Fig. 9 Comparison of punch stroke-force of simulated S5 from Nakazima test with experimental test [23]

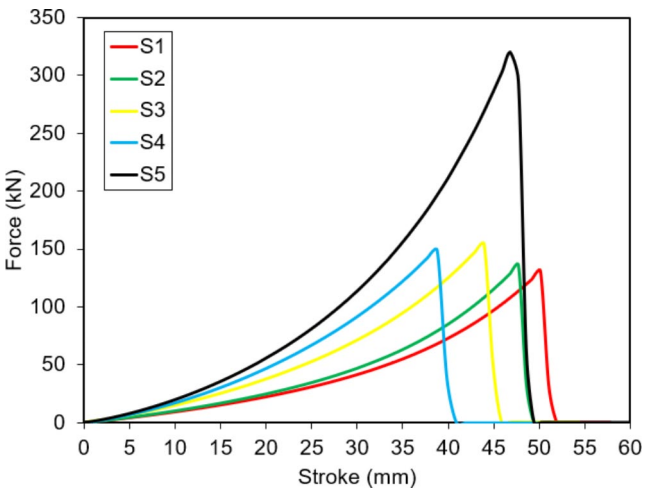

Fig. 10 Nakazima specimens stroke force punch profiles

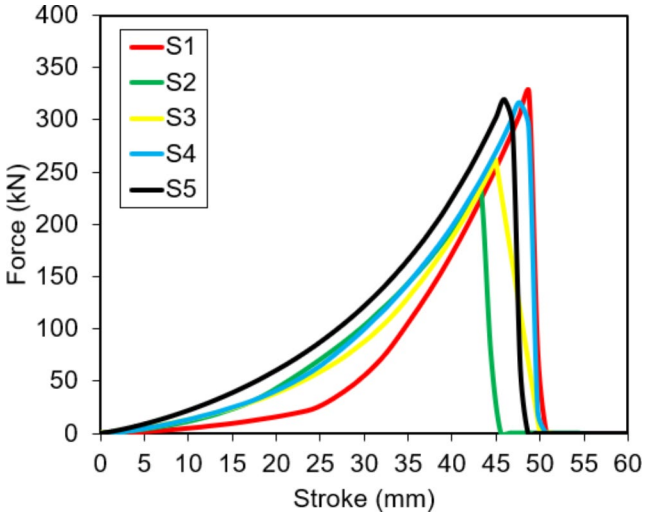

Fig. 11 Banabic modified specimens stroke force punch profile

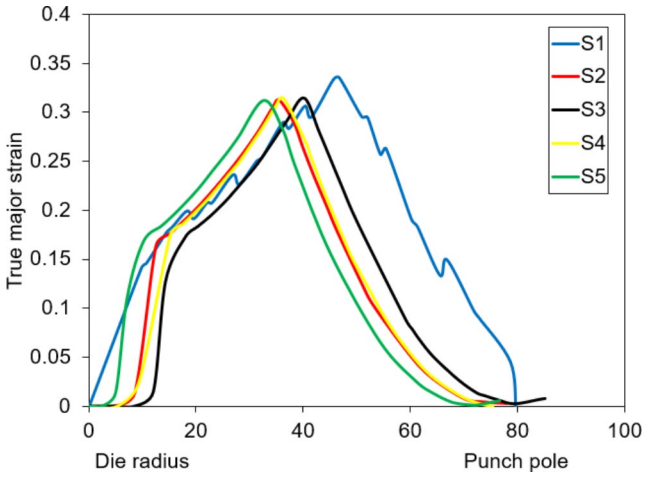

Fig. 12 Strain profiles of Nakazima test specimens

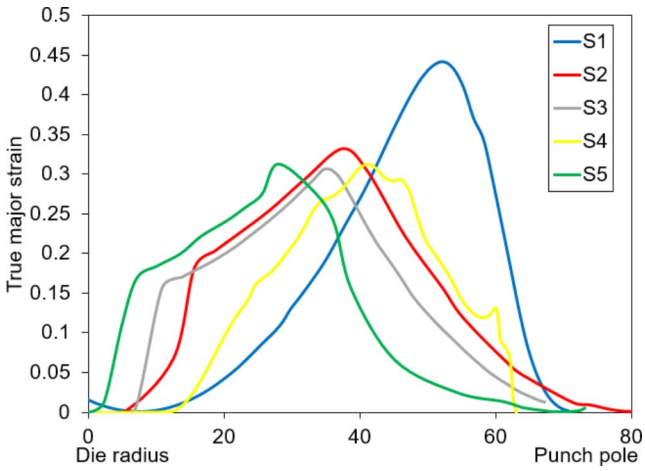

Fig. 13 Strain profiles of Banabic modified test specimen

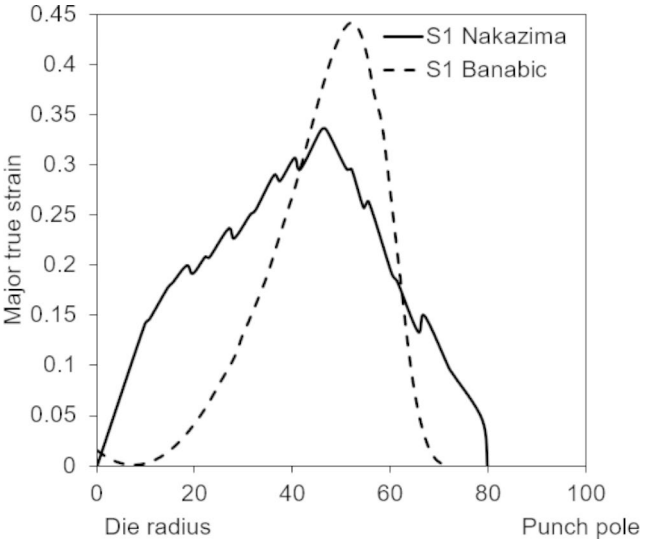

Fig. 14 Strain profile of specimens 1 of Nakazima and Banabic modified methods

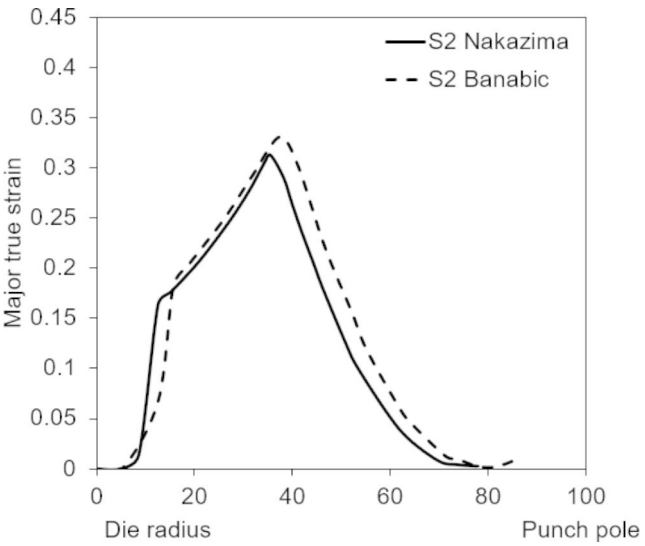

Fig. 15 Strain profile of specimens 2 of Nakazima and Banabic modified methods

these methods, the S2 due to the presence of a smaller proportion of uniaxial strain, with the emergence of the plane strain state, the maximum value of the greatest true strain tends to decrease.

As can be seen in Fig. 16, the strain profile of the S3 of the Nakazima method presented a true greatest strain peak of 0.325, which was higher when compared to the adapted Banabic, which resulted in 0.3, which predominantly present the plane strain state. Unlike specimens S1 and S2, the highest strains of the specimens of Nakazima occurred closer to the punch pole between both.

The strain profiles of the S4 are illustrated in Fig. 17 which present as predominant the states of plane strain and

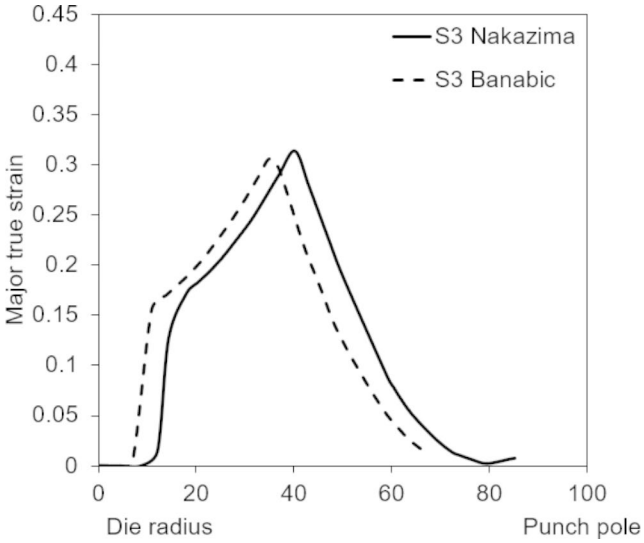

Fig. 16 Strain profile of specimens 3 of Nakazima and Banabic modified methods

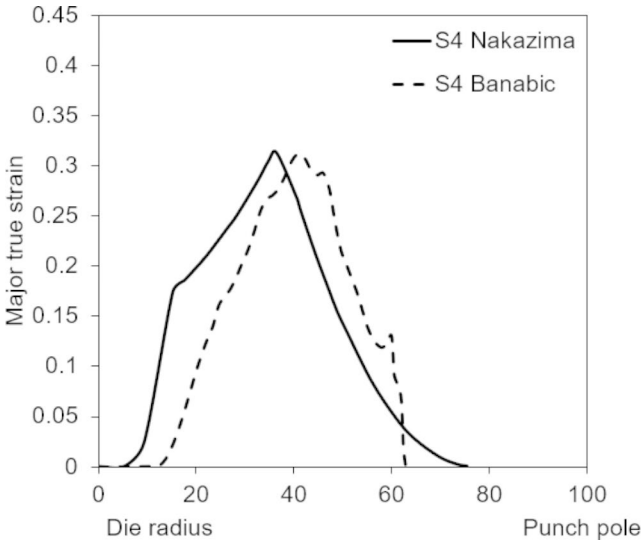

Fig. 17 Strain profile of specimens 4 of Nakazima and Banabic modified methods

stretching. The adapted specimen of Banabic presented the strain peak closer to the punch pole than the one of Nakazima, but the difference between the peaks of both was low, being 0.325 and 0.323.

4 Conclusion

The numerical simulations were successfully performed using the method that consisted of defining the mechanical properties and failure criteria of the DP 600 steel in the Abaqus software, taken from the experimental tests by Chemin Filho [23]. By calibrating the tribological parameters, the results were close to the experimental values obtained by Chemin Filho at the time of model validation with S5. It was possible to verify that the specimens of the adapted Banabic test present better performance in DP 600 steels when compared to those used in the Nakazima method. This was due to their geometries providing greater strain, stress distribution and maximum strain values closer to the punch pole in their specimens. The Banabic method that has been adapted by modifying the size of the specimens can follow the standards of DIN EN ISO 12004-2 during practical tests. However, experimental tests must be carried out and employ the conformation limits resulting from this test in practical utility applications in order to prove this condition. The preparation of specimens for the Banabic test is simpler than for the Nakazima test, when the DIN EN ISO 12004-2 standard is followed. These geometries have more machinability since the ends do not have the need to produce notches on the sides, a condition that facilitates fixing, produces less distortion on the edges, consequently producing less work hardening and influencing the results.

Supplementary information The online version contains supplementary material available at https://doi.org/10.1007/s12008-023-01218-7.

References

1. Roy, T.K., Bhattacharya, B., Ghosh, C., Ajmani, S.K.: Advanced high Strength Steel. Springer Nature Singapore Pte Ltd, New York (2018)
2. Keeler, S., Kimchi, M.: Advanced High-Strength Steels Application Guidelines Version 6.0. 3S-Superior Stamping Solutions. *LLC., WorldAutoSteel*, 1–17. (2017)
3. Demeri, M.Y.: Advanced high-strength Steels: Science, Technology, and Applications. ASM international (2013)
4. Marcondes, P.V.P., dos Santos, R.A., Haus, S.A.: The coining force influence on springback in TRIP800 steel V and L-bending processes. J. Brazilian Soc. Mech. Sci. Eng. **38**(2), 455–463 (2016)
5. Ashby, M.F., Jones, D.R.: Engineering Materials 1: An Introduction to Properties, Applications and Design, vol. 1. Elsevier (2011)
6. Giansoldati, M., Monte, A., Scorrano, M.: Barriers to the adoption of electric cars: evidence from an italian survey. Energy Policy. **146**, 111812 (2020)
7. Stahl, W.W., Bućko, P.: Analysis of the impact of charging electric cars on the power system load.Acta Energetica. (2019)
8. Harlow, S.: Lithium war heats up after epic launch of tesla model. Oilprice.com. London, 19 abr. (2016)
9. Kuziak, R., Kawalla, R., Waengler, S.: Advanced high strength steels for automotive industry. Archives of civil and mechanical engineering. **8**(2), 103–117 (2008)
10. Soleimani, M., Mirzadeh, H., Dehghanian, C.: Processing route effects on the mechanical and corrosion properties of dual phase steel. Met. Mater. Int. **26**(6), 882–890 (2020)
11. Tasan, C.C., Diehl, M., Yan, D., Bechtold, M., Roters, F., Schemmann, L., Zheng, C., Peranio, N., Ponge, D., Koyama, M., Tsuzaki, K.: An overview of dual-phase steels: advances

in microstructure-oriented processing and micromechanically guided design. Annu. Rev. Mater. Sci. **45**, 391–431 (2015)
12. Nikhare, C., Hodgson, P.D., Weiss, M.: Necking and fracture of advanced high strength steels. Mater. Sci. Engineering: A. **528**(6), 3010–3013 (2011)
13. Waterschoot, T., Verbeken, K., BC, D.C.: Tempering kinetics of the martensitic phase in DP steel. ISIJ Int. **46**(1), 138–146 (2006)
14. Panich, S., Barlat, F., Uthaisangsuk, V., Suranuntchai, S., Jirathearanat, S.: Experimental and theoretical formability analysis using strain and stress based forming limit diagram for advanced high strength steels. Mater. Design. **51**, 756–766 (2013)
15. Abspoel, M., Scholting, M.E., Droog, J.M.: A new method for predicting forming limit curves from mechanical properties. J. Mater. Process. Technol. **213**(5), 759–769 (2013)
16. Banabic, D., Lazarescu, L., Paraianu, L., Ciobanu, I., Nicodim, I., Comsa, D.S.: Development of a new procedure for the experimental determination of the forming limit curves. CIRP Ann. **62**(1), 255–258 (2013)
17. Keeler, S.P.: *Plastic instability and fracture in sheets stretched over rigid punches* (Doctoral dissertation, Massachusetts Institute of Technology). (1961)
18. Goodwin, G.M.: Application of strain analysis to sheet metal forming problems in the press shop.Sae Transactions,380–387. (1968)
19. Gipiela, M.L., Fabris, A., Marcondes, P.V.P.: Influencia da força do prensa-chapas na Conformabilidade do aço multifásico CPW 800. Congresso Nacional De Engenharia Mecânica,Uberlândia (2014)
20. Hecker, S.: Formability of aluminum alloy sheets. J. Eng. Mater. Technol. v. **97**(1), 66–73 (1975)
21. Brazilian Technical Standards Association. NBR 6673: Produtos Planos de Aço—Determinação das Propriedades Mecânicas a Tração. (1981)
22. ISO, D.: Metallic materials-Sheet and strip-Determination of forming-limit curves-Part 2: Determination of forming-limit curves in the laboratory. *ISO*. (2008)
23. Chemin Filho, R.A.: Estudo da fratura de aços de nova geração DP600 através da variação de pressão no prensa-chapas. (2011)
24. Madi, M., Júnior, M.V., Marcondes, P.V.P.: An analysis of the forming speed variation with relation to deep drawing depth of steel DP 600 sheets. Int. J. Adv. Manuf. Technol. **99**(9), 2417–2424 (2018)
25. Valente Tigrinho, L.M., Filho, C., R. A., Prestes Marcondes, P.V.: Fracture analysis approach of DP600 steel when subjected to different stress/strain states during deformation. Int. J. Adv. Manuf. Technol. **69**(5), 1017–1024 (2013)